Mechanical properties and pattern collapse of chemically amplified photoresists

Long Que and Yogesh B. Gianchandani[a)]
Center for Nano Technology, Department of Electrical and Computer Engineering, University of Wisconsin, 1415 Engineering Drive, Madison, Wisconsin 53706

(Received 1 June 2000; accepted 25 August 2000)

The mechanical properties of positive tone chemically amplified resists UV6 and APEX-E are measured and used in finite element analysis (FEA) to determine the mechanical compliance of photoresist lines as an indicator of the propensity for pattern collapse. Specifically, the residual strain is determined by surface micromachined resist structures; the residual stress, expansion coefficient, and glass transition temperatures are determined from wafer curvature measurements; and the Young's modulus is calculated from the stress and strain. The results indicate that UV-6 has higher strain and a higher coefficient of thermal expansion than APEX-E. However, it has lower residual stress because its Young's modulus is 50%–70% lower than that of APEX-E. FEA indicates that lines of UV6 have greater compliance than those of APEX-E, and are more easily deformed by fluidic forces during develop and rinse steps. This is fully consistent with separate reports that demonstrate a greater likelihood of pattern collapse in UV6 than APEX-E. © *2000 American Vacuum Society.* [S0734-211X(00)08706-0]

I. INTRODUCTION

The progressive reduction of linewidths in lithography has led to increasing thickness-to-width aspect ratios in photoresist features,[1] requiring them to be treated as three-dimensional mechanical structures for modeling failure modes. For example, evidence suggests that residual strain may play a significant role in pattern distortion and resist delamination in sub-100/nm features,[2,3] exacerbating problems caused by the forces in rinsing and drying. One mode of failure is caused by the lateral deflection of the top surfaces of two adjacent lines of photoresist to the extent that they touch each other. They may remain in contact even after the wafer is removed from the rinse and dried, resulting in a lithography defect. For a better understanding of scaling limits in lithography, the mechanical properties of the resist, such as the Young's modulus, residual strain, residual stress, coefficient of thermal expansion (CTE), and the glass transition temperature (T_g), are needed. Once these properties are determined, the mechanical deformations of resist structures which occur as a consequence of various forces encountered in processing can be calculated. In this effort, we report on measurements of these five properties for the chemically amplified positive tone Shipley resists UV6 and APEX-E and evaluate the lateral compliance of patterned photoresist lines using finite element analysis (FEA) as an indicator of their propensity for collapse.

II. EXPERIMENTAL RESULTS

The measurements of residual strain and subsequent calculations of Young's modulus were facilitated by micromachined strain sensors that were fabricated using the resist as a structural material. Bent beam strain sensors are small, highly sensitive microstructures that are simple to fabricate, and provide high linearity and wide dynamic range.[4,5] Each device consists of a pair of V-shaped suspended beams, with a vernier located at the apex (Fig. 1). When the beams are released from the substrate by selectively etching away the underlying sacrificial material, the residual strain in the structural material, in this case photoresist, displaces the apices, and can be read by the vernier. Device response is tailored by adjusting the length, width, and bending angle of the beams. For example, a device of 200 μm length, 1.5 μm width, and 0.2 radian bending angle, using a vernier with ± 2 μm range and 0.1 μm resolution, provides 100 μstrain resolution over a range of ± 2000 μstrain.

The strain sensors were fabricated by a surface micromachining process using a single lithography step. A Ti sacrificial layer was first deposited on the Si substrate, followed by structural photoresist which was processed and patterned as described in Table I. The sacrificial layer was then selectively etched away by a timed wet etch, releasing the beams and verniers from the substrate while leaving the anchors attached. Vernier displacements were recorded using a microscope without removing the sample from the final rinse

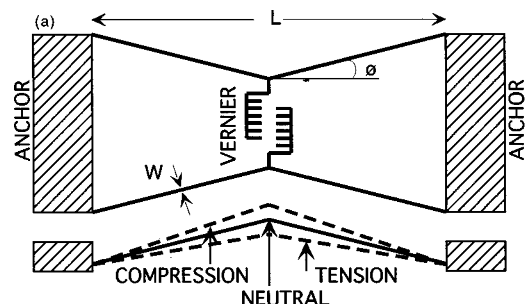

FIG. 1. Schematic of the bent-beam strain sensor.

[a)]Author to whom all correspondence should be addressed; electronic mail: yogesh@engr.wisc.edu

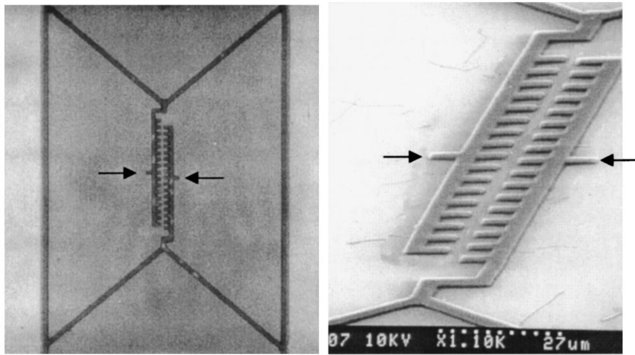

FIG. 2. Optical micrograph (right-hand side) and a scanning electron microscope image (left-hand side) of a fabricated strain sensor using resist as the structural material. Misalignment of the verniers, indicated by arrows, quantifies the residual strain in the resist.

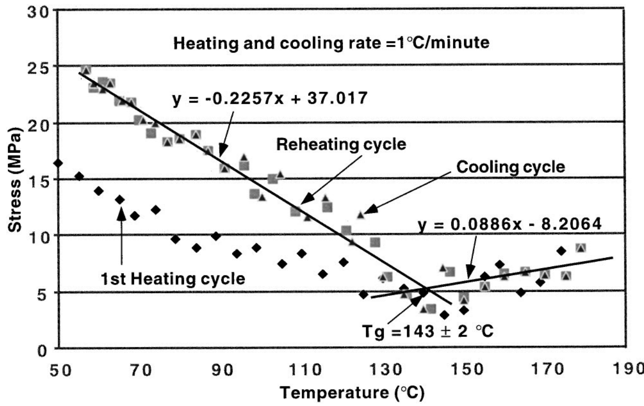

FIG. 3. Measurements show that although the stress–temperature relationship of UV6 is altered by chemical reaction in the first heating ramp, subsequent cooling, and heating cycles track each other. Using these, the T_g is determined to be 143.0±2.5 °C and CTE (below 143 °C) is 34.9 ±2.3 ppm/K.

TABLE I. Fabrication sequence for strain measurements.

Parameter	UV6	APEX-E
Batch No.	BH4411	YJ4388
Spin speed/No. coatings	1000 rpm/two	1000 and 1500 rpm/one
Resist thickness (final)	1.34±0.02 μm	0.7, 1.1 μm
PAB time/temp.	60 s/130 °C	120 s/85 °C
Exposure dose	18 μC/cm^2	4.5 μC/cm^2
PEB time/temp.	90 s/130 °C	120 180 s/85 °C
Develop	MF 320, 60 s	MF 320, 60 s
Final strain (wet)	1410±300 μstrain (Unexposed resist)	670±20 μstrain (Unexposed resist)

TABLE II. Fabrication sequence for stress measurements.

Parameter	UV6	APEX-E
Batch No.	BH4411	YJ4388
Spin speed/No. coatings	1000 rpm/two	2000 rpm/two
Resist thickness-1	27 740±20 Å	8677±210 Å
Resist stress-1	4.5–5.0 MPa	9.9–10.4 MPa
PAB time/temp.	60 s/130 °C	120 s/85 °C
Resist thickness-2	14 450±20 Å	7,498±10 Å
Resist stress-2	8.5–9.2 MPa	15.5–16.1 MPa
Exposure	None	None
PEB time/temp.	90 s/130 °C	120 s/85 °C
Resist thickness-3	13 960±20 Å	7439±10 Å
Resist stress-3	10.2–11.0 MPa	16.5–117.0 MPa
Develop and nitrogen dry	MF 320, 60 s	MF 320, 60 s
Resist thickness-4	13 420±20 Å	7290±210 Å
Resist stress-4	10.0±0.2 MPa	14.5±0.1 MPa

water. This eliminated the possibility of device deformation due to capillary forces exerted on the structure while drying the sample. Micrographs of a fabricated device are shown in Fig. 2, with the misaligned verniers indicating a tensile stress. Measured results indicate that wet UV6 was in 1410 ±300 μstrain tension, whereas APEX-E was in 670 ±20 μstrain tension for the conditions tested.

The residual stress of each resist was measured by determining the change that it caused in the curvature of the substrate wafer as measured by a laser-based tool.[6,7] The resist was processed in a manner similar to the strain sensors (Table II). The measurements showed that UV6 was in 10.0±0.2 MPa tension whereas APEX-E was in 14.5 ±0.1 MPa tension at ambient temperature. The ratio of measured stress to strain provided the Young's modulus at room temperature, yielding 7.0±0.5 GPa for UV6, and 21.5 ±5.0 GPa for APEX-E. As the temperature was raised, the stress reduced. The thermal stress in the resist film is proportional to the difference between its thermal expansion coefficient and that of the substrate. Since the thermal expansion coefficient of the resist is a constant below its T_g, the stress

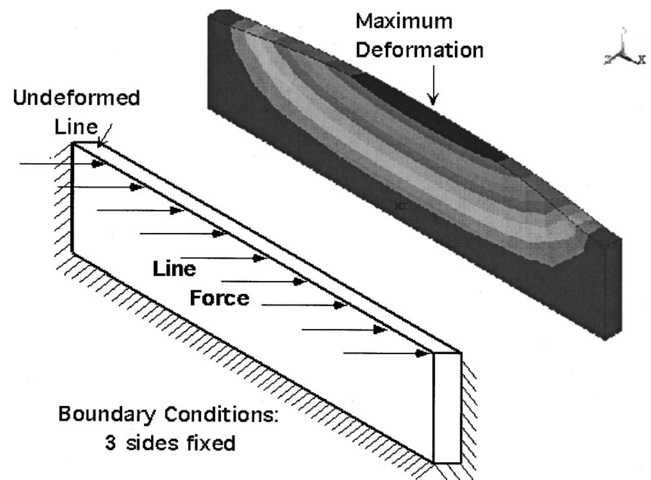

FIG. 4. Schematic of the solid model used for FEA, and a contour plot of the calculated deformations.

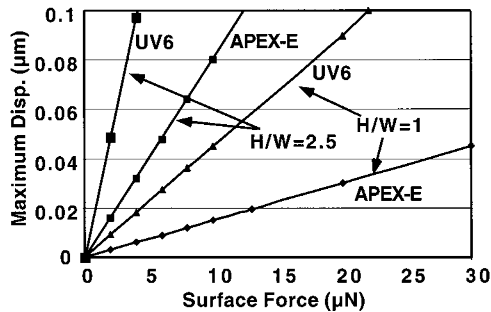

FIG. 5. Comparison of maximum lateral deflection in 5 μm long APEX-E and UV6 lines with 0.2 μm linewidths and 5:2 and 1:1 height-to-width aspect ratios. Lower compliance of APEX-E lines suggests that they are more resistant to collapse.

may be expected to change linearly with temperature. In the experiments, the first heating ramp showed some nonlinearity which may be caused by structural changes in the resist (Fig. 3). One possible explanation is that the free volume that is lost in the polymer as the temperature increases cannot be recovered once the resist begins to reflow in the vicinity of T_g.[8] Subsequent cooling and reheating cycles showed a linear relationship (Fig. 3). The slope of this line provided the CTE for resist, yielding 34.9 ± 2.3 ppm/K for UV6 and 11.0 ± 2.5 ppm/K for APEX-E in the manner identified in Ref. 7. As the temperature continued to rise, however, the linearity was eventually lost at T_g, at which the thermal expansion coefficient of the photoresist changes due to the phase transition.[8] This temperature was found to be 143.0 ± 2.5 °C for UV6 (Fig. 3), and 118 ± 2 °C for APEX-E.[5] It should be noted that 1 °C/min heating and cooling rate was used to permit thermal equilibrium to be established for each data point. All the mechanical properties determined for both resists as a result of these experiments are summarized in Table III.

In summary, the measurements indicate that UV-6 has higher strain and a higher coefficient of thermal expansion than APEX-E. However, it has lower residual stress because its Young's modulus is 50%–70% lower than that of APEX-E.

III. ANALYSIS AND CONCLUSIONS

It is known[2,3,9] that uneven fluidic forces associated with the postdevelop rinse contribute to collapse in resist lines. One factor that contributes to the propensity for collapse is the lateral compliance of a line, which can be modeled by FEA given the material properties that are available from the preceding measurements. Lateral deflections of 5 μm long photoresist lines with 0.2 μm width and thickness: width aspect ratios of 1:1 and 5:2 were compared. A loading force was applied in a uniformly distributed manner along the top edge of the structure, as shown in Fig. 4. The displacement of the bottom and side surfaces was constrained to zero by boundary conditions, and the maximum lateral displacement was obtained as shown in the contour plot in Fig. 4. The variation of the maximum displacement with applied force for the four structures simulated is shown in Fig. 5. The lateral compliance is inversely related to the slope of the lines in this figure. Clearly, APEX-E lines show smaller deflections, suggesting a lower likelihood of collapse. As expected, lines with larger thickness: width aspect ratios also show greater lateral compliance. These trends are both in full agreement with experimental results on resist collapse that were recently reported by Cao and Nealey.[9]

TABLE III. Summary of measured properties.

Property	UV6	APEX-E
Residual strain (RT)	1410 ± 300 μstrain	670 ± 20 μstrain
Residual stress (RT)	10.0 ± 0.2 MPa	14.5 ± 0.1 MPa
Young's modulus (RT)	7.0 ± 0.5 GPa	21.5 ± 5.0 GPa
Coeff. of thermal expansion	34.9 ± 2.3 ppm/K	11.0 ± 2.5 ppm/K
Glass transition temperature	143.0 ± 2.5 °C	118.0 ± 2.0 °C

In conclusion, we note that by combining a material characterization technique that uses simple microstructures with a conventional wafer curvature measurement technique, the stress, strain, Young's modulus, thermal expansion coefficient, and T_g of a photoresist can be rapidly characterized. The values determined for APEX-E and UV6 are summarized in Table III. FEA can then be used to predict trends in pattern collapse.

ACKNOWLEDGMENTS

The authors thank Jaz Bansel for help with e-beam lithography, Professor Paul Nealey for correlating the FEA results with data on photoresist collapse, and Professor Franco Cerrina for discussions. This work was funded in part by the Semiconductor Research Corporation Contract No. 98-LP-452.005. The Center for NanoTechnology, University of Wisconsin–Madison, is supported in part by DARPA/ONR Grant No. N00014-97-1-0460. The Synchrotron Radiation Center of University of Wisconsin–Madison, at which some of the experimental facilities are located, is operated under NSF Award No. DMR-95-31009

[1] H. H. Solak, D. He, W. Li, and F. Cerrina, J. Vac. Sci. Technol. B **17**, 3052 (1999).
[2] S. Mori, T. Morisawa, N. Matsuzawa, Y. Kaimoto, M. Endo, T. Matsuo, and M. Sasago, J. Vac. Sci. Technol. B **16**, 3744 (1998).
[3] Z. G. Chen, Ph.D. thesis, University of Wisconsin–Madison, 1998.
[4] Y. B. Gianchandani and K. Najafi, J. Microelectromech. Syst. **5**, 52 (1996).
[5] L. Que, Y. Gianchandani, and F. Cerrina, J. Vac. Sci. Technol. B **17**, 2719 (1999).
[6] Tencor™ FLX-2320 User Manual, KLA-Tencor Corporation, San Jose, CA, 1995.
[7] J. F. Gaynor and S. B. Desu, J. Mater. Sci. Lett. **13**, 236 (1994).
[8] T. G. Fox and P. J. Flory, J. Appl. Phys. **21**, 581 (1950).
[9] H. Cao, J. J. de Pablo, and P. M. Nealey (submitted).